

The luminescent quantum efficiency of Eu^{2+} ions in alkali halides determined by simultaneous multiwavelength photoacoustic and luminescence experiments

This article has been downloaded from IOPscience. Please scroll down to see the full text article.

1994 J. Phys.: Condens. Matter 6 10625

(<http://iopscience.iop.org/0953-8984/6/48/021>)

View [the table of contents for this issue](#), or go to the [journal homepage](#) for more

Download details:

IP Address: 171.66.16.179

The article was downloaded on 13/05/2010 at 11:28

Please note that [terms and conditions apply](#).

The luminescent quantum efficiency of Eu^{2+} ions in alkali halides determined by simultaneous multiwavelength photoacoustic and luminescence experiments

E Rodríguez†, J A Muñoz‡, J O Tocho§ and F Cussó†

† AT& T-ME, Polígono Industrial Zona Oeste, Tres Cantos, 28760 Madrid, Spain

‡ Departamento de Física de Materiales, C-IV, Universidad Autónoma de Madrid, 28049 Madrid, Spain

§ Centro de Investigaciones Ópticas, La Plata, Argentina

Received 4 July 1994, in final form 14 September 1994

Abstract. In this work, the luminescent quantum efficiency of Eu^{2+} ions in alkali halides is determined by using a method based on the simultaneous and multiwavelength measurement of photoacoustic and luminescent signals after pulsed laser excitation. This method, which was first demonstrated in Eu^{2+} -doped KCl, is now extended in order to include the possibility of direct non-radiative relaxation from upper excited states to the ground state. A high quantum efficiency is found for Eu^{2+} ions in different alkali halides (NaCl, KCl, KBr and KI).

1. Introduction

The quantum efficiency (Φ) of a luminescent material is obviously one of its most relevant parameters. Photoacoustic methods have been extensively used in the quantum efficiency determination of gases and liquid materials [1–3]. In these cases it becomes relatively easy to change concentrations or compositions, relating the photoacoustic signal of the sample to that of a standard material with known quantum efficiency.

For solid state materials, and with the limited exceptions where photochemical transformations may be induced *in situ* [4], changing concentrations implies changing the sample. This procedure is not adequate for quantitative measurements, because of the fact that changing the sample may substantially affect the acoustic coupling in the experimental chamber.

Some authors have pointed out the possibility of obtaining absolute measurements without standards [5, 6] and, recently, an alternative method based on the simultaneous detection of photoacoustic and luminescent signals, after excitation at different wavelengths, has been proposed [7]. This method relies on the existence of a non-radiative relaxation, providing an internal reference that can be used for absolute quantum efficiency determination.

This method was first applied to the determination of the luminescent quantum efficiency of Eu^{2+} ions in KCl [7], a system which meets all the conditions required (two broad absorption bands, suitable for laser excitation, non-radiatively connected and having a single luminescent emission). In this first analysis, and assuming 100% non-radiative internal relaxation, it has been found that the Eu^{2+} ions exhibit nearly 100% luminescent efficiency confirming their possibilities as active ions in many phosphor materials.

The assumption of a fully non-radiative relaxation between excited states, which was previously adopted in the analysis of KCl:Eu²⁺ [7], may lead to an overestimation of the quantum efficiency. In this work we present the extension of the above mentioned method to a more general case, where the relaxation from the upper excited state to the ground state is also possible. This extended analysis is applied to the determination of the Eu²⁺ luminescence quantum efficiency in different alkali halide hosts (NaCl, KCl, KBr and KI).

The knowledge of the luminescent quantum efficiency of Eu²⁺ ions in these materials becomes necessary to understand and evaluate the possibilities of recently proposed applications, such as their use as active ions in ultraviolet (UV) detection, either by directly using its luminescent emission [8] or as a UV activated thermoluminescent material [9].

2. Experimental set-up

The crystals used in this work were grown, by the Czochralski method, in the Crystal Growth Laboratory of the Universidad Autónoma de Madrid. The concentration of Eu²⁺ ions in the crystals, expressed in parts per million (ppm), as determined from the absorption spectrum and calibrated cross-sections [10], were 140, 280, 570 and 290 ppm for NaCl, KCl, KBr and KI respectively.

Samples, in the form of a rectangular slabs of approximate dimensions $10 \times 5 \times 1 \text{ mm}^3$, were cut from the boules. In order to suppress Eu²⁺ aggregates and/or precipitates, the samples were annealed for 30 min at 600 °C and then quenched to room temperature on a Cu block prior to the measurements.

Optical absorption and luminescence measurements were performed by using a Cary 14 spectrophotometer and a Jobin-Yvon JY3CS spectrofluorimeter.

Pulsed excitation, at different wavelengths, is achieved by using an Nd:YAG laser (Quanta Ray DCR-2) linked to a harmonics generator. The laser gives 10 ns pulses with energies ranging from 300 mJ in the infrared (1.064 μm) to 20 mJ in the UV (266 nm).

The piezoelectric transducer was glued to one edge of the sample and the luminescence was collected from the opposite edge with an optical fibre coupled to the entrance slit of a monochromator before reaching the photomultiplier, while the excitation was performed through the larger case of the sample.

Photoacoustic and luminescent signals were detected simultaneously using a resonant piezoelectric transducer having a bandwidth of 200 kHz [11], and an EMI 9558QB photomultiplier tube. Both signals were suitably amplified and finally averaged and recorded using a digital oscilloscope (Tektronix 420).

3. Experimental results and discussion

The absorption spectra of Eu²⁺ ions in alkali halide crystals consist of two broad absorption bands attributed to transitions from the $^8S_{7/2}$ ground state of the $4f^7$ configuration to the $4f^65d$ configuration [12]. In cubic symmetry, the crystal field splits the d-electron state into two components, e_g and t_{2g} , which correspond to the observed absorption bands (figure 1). For sixfold coordination, which is the case for Eu²⁺ ions entering substitutionally for the alkali ions, the t_{2g} is the low-lying level.

As has been indicated in figure 1(a), the two Eu²⁺ absorption bands can be excited with the third ($3\omega_0$) and fourth ($4\omega_0$) harmonics of the Nd:YAG laser at $\lambda = 355 \text{ nm}$ and $\lambda = 266 \text{ nm}$ respectively. After excitation within either of these two bands a single luminescence band is observed, corresponding to the $t_{2g} \rightarrow 4f^7$ transition.

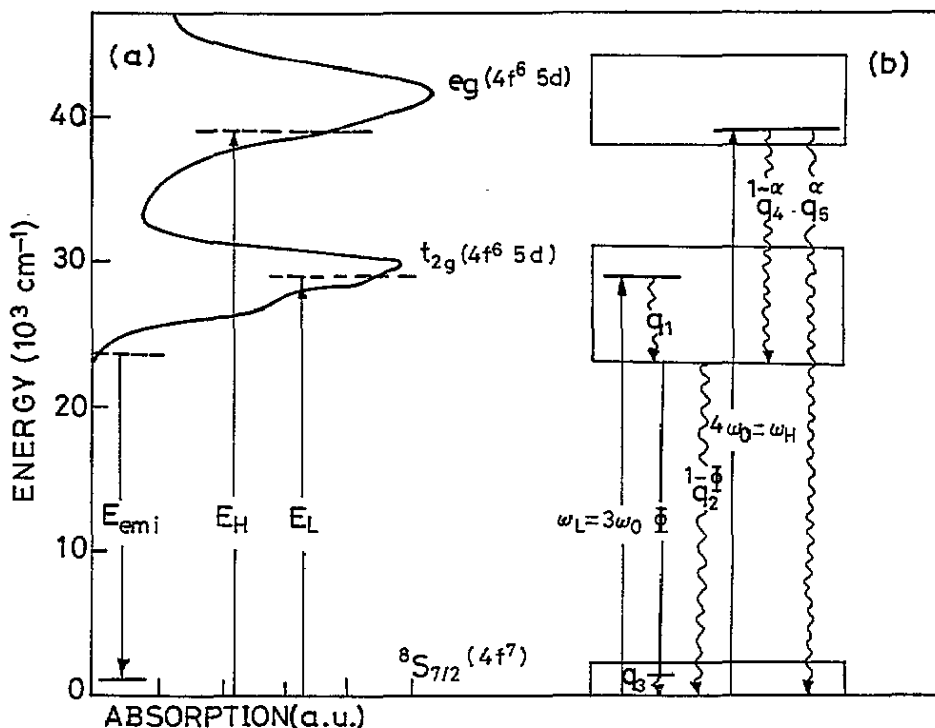


Figure 1. (a) The absorption bands of Eu^{2+} in alkali halides, showing the coincidence with the third ($3\omega_0$) and fourth ($4\omega_0$) harmonics of the Nd:YAG laser. (b) A schematic energy diagram indicating the different contributions to the photoacoustic and luminescent signals.

The detailed properties of the Eu^{2+} luminescence are slightly dependent on the host matrix [12], and for freshly quenched samples of NaCl, KCl, KBr and KI the emission bands have their maxima at 427 nm, 419 nm, 428 nm and 427 nm respectively. It is important to remark that in all matrices the same emission is detected after excitation to the high- (e_g) or low- (t_{2g}) energy state.

After pulsed excitation, the luminescence decays exponentially after a fast rise, coincident with the excitation time, while the photoacoustic signal, which consists of a series of compressions and expansions, gives rise in the transducer to an oscillating signal delayed from the excitation because of the time the acoustic signal needs to reach the piezoelectric transducer. The temporal maxima of both luminescent (LUM) and photoacoustic (PAS) signals are a measure of the intensities generated in these processes. (In the case of photoacoustic measurements, the first maximum, which is the least influenced by reflections, will be taken).

The simplified energy-level scheme of figure 1(b), where the different contributions to the luminescent or photoacoustic signals are indicated, will be used to interpret the observed results. Considering first the excitation to the lower excited state (t_{2g} level) at a frequency of $\omega_L = 3\omega_0$, the non-radiative relaxation within this level gives a thermal contribution q_1 . The relaxation from the bottom of this lower excited state to the $4f^7$ level is assumed to be luminescent with a quantum efficiency Φ , followed by a non-radiative relaxation within the ground state with a thermal contribution Φq_3 . The non-radiative channel gives also a contribution $(1 - \Phi)q_2$.

In the case of excitation to the upper excited state (e_g level) at a frequency $\omega_H = 4\omega_0$,

two different de-excitation channels appear. A first one, fully non-radiative from this level to the ground state with a probability α , gives a thermal contribution αq_5 . A second one implies a decay to the lower excited state (with a thermal contribution $((1-\alpha)q_4)$) followed by the luminescent process described above.

Taking into account these contributions, the dependence of the luminescent (LUM) and photoacoustic (PAS) signals on the number of absorbed photons can be expressed as

$$\text{LUM}(\omega_L) = K_L \Phi N_a(\omega_L) \quad (1a)$$

$$\text{LUM}(\omega_H) = K_L \Phi N_a(\omega_H)(1 - \alpha) \quad (1b)$$

$$\text{PAS}(\omega_L) = K_P[q_1 + (1 - \Phi)q_2 + \Phi q_3]N_a(\omega_L) \quad (2a)$$

$$\text{PAS}(\omega_H) = K_P[q_5\alpha + (1 - \alpha)(q_4 + (1 - \Phi)q_2 + q_3\Phi)]N_a(\omega_H) \quad (2b)$$

where $N_a(\omega_L, \omega_H)$ indicates the number of absorbed photons at the corresponding wavelength and K_L and K_P are proportionality constants that include all the instrumental responses involved in the collection of luminescent and photoacoustic signals.

Although the energy difference between the upper excited state and the ground state is quite high, which may induce neglect of the probability of direct non-radiative relaxation ($\alpha = 0$), this is not justifiable in general.

In fact, this can be verified experimentally by comparing the luminescent signals after excitation to the upper or lower excited states. From equations (1a) and (1b) the fraction of excited ions that decay via the lower excited state, $(1 - \alpha)$, is readily expressed as

$$1 - \alpha = \frac{\partial \text{LUM}(\omega_H) / \partial N_a(\omega_H)}{\partial \text{LUM}(\omega_L) / \partial N_a(\omega_L)} \quad (3)$$

The values obtained from equation (3) for Eu^{2+} ions in NaCl, KCl, KBr and KI are summarized in table 1.

It can be observed that, although not very important in freshly quenched samples, there is a fraction ($0.05 \leq \alpha \leq 0.09$) of ions excited to the upper energy state that decay non-radiatively to the ground state. The omission of this contribution, assuming $\alpha = 0$, slightly overestimates the value of the quantum efficiency by a few per cent [7].

The luminescent quantum efficiency may now be obtained by comparing the photoacoustic signals after excitation at ω_L and ω_H (equations (2a) and (2b)). However, a better approach is to compare directly the photoacoustic and luminescent signals generated at different excitation powers for each excitation wavelength.

As both the photoacoustic and luminescent signals are directly proportional to the number of absorbed photons, $N_a(3\omega, 4\omega)$, it is possible to eliminate between equations (1) and (2) the dependence on $N_a(3\omega, 4\omega)$. In this way the accuracy of the method is enhanced, avoiding the uncertainties in the measurement of the number of absorbed photons.

In terms of the energies involved in the process (see figure 1), E_H, E_L, E_{emi} , the following expressions are readily obtained:

$$\text{PAS}(\omega_L) = (K_P/K_L)[(E_L - E_{\text{emi}}\Phi)/\Phi]\text{LUM}(\omega_L) \quad (4a)$$

$$\text{PAS}(\omega_H) = (K_P/K_L)\{[E_H - E_{\text{emi}}(1 - \alpha)\Phi]/\Phi(1 - \alpha)\}\text{LUM}(\omega_H). \quad (4b)$$

The experimentally dependent constants appear as the quotient (K_P/K_L) , and they can be eliminated by comparing (4a) and (4b). This leads to an explicit expression for the

quantum efficiency in terms of the excitation (ω_L, ω_H) and emission (ω_{emi}) frequencies and the quantity Λ , defined in equation (5) below, which is a parameter to be determined experimentally.

$$\Lambda = [\partial \text{PAS}(\omega_H) / \partial \text{LUM}(\omega_H)] / [\partial \text{PAS}(\omega_L) / \partial \text{LUM}(\omega_L)] \quad (5)$$

$$\Phi = (\omega_L / \omega_{\text{emi}}) [\Lambda - (\omega_H / \omega_L) / (1 - \alpha)] / (\Lambda - 1). \quad (6)$$

The comparison of photoacoustic signal versus luminescence for NaCl, KCl, KBr and KI crystals is presented in figure 2. A linear dependence, as expected from equations (4), is observed in all cases at the excitation powers used in this work (no multiphoton processes or excited state absorption is involved [13]).

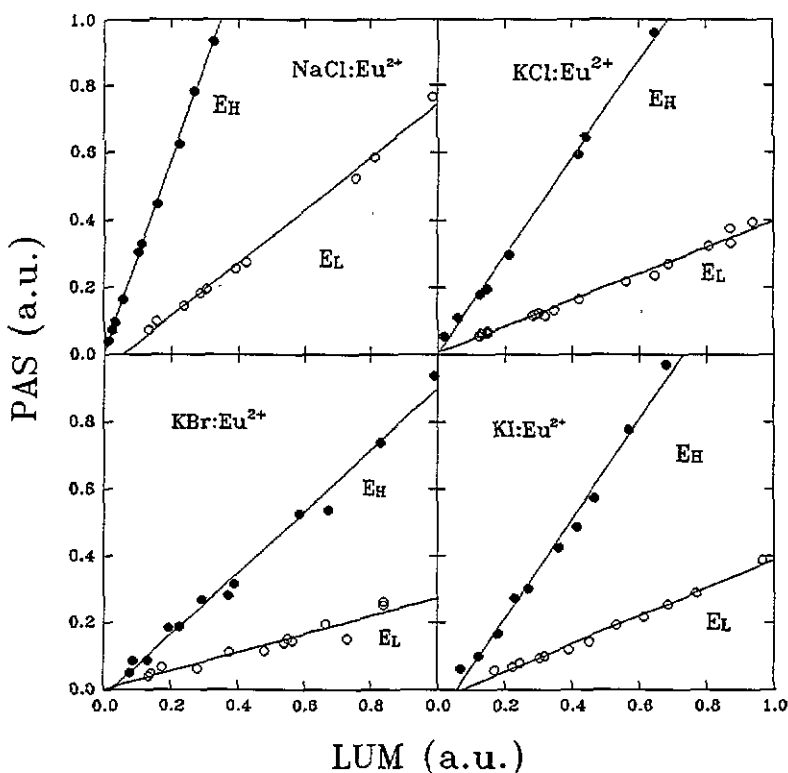


Figure 2. A comparison of the photoacoustic (PAS) and luminescent (LUM) signals simultaneously generated after $3\omega_H$ (full circles) and $4\omega_L$ (open circles) excitation of Eu^{2+} in NaCl, KCl, KBr and KI crystals.

The difference in slope between ω_H and ω_L excitation, a consequence of the non-radiative connection between the excited states of Eu^{2+} ions, is apparent.

An analysis of this method shows that the higher the difference in slope (Λ) the higher the precision in the determination of the quantum efficiency Φ . This is a consequence of increasing the relative magnitude of the internal non-radiative relaxation used as calibration [14].

With the values of Λ obtained from the least-squares fitting of slopes of PAS against LUM for ω_H and ω_L of figure 2, together with the values of α previously determined, the luminescent quantum efficiency, Φ , is calculated and is given in table 1. From the experimental standard deviation of Λ and α values, and their propagation using equation (6), the accuracy in the quantum efficiency $\Delta\Phi$ has been calculated and is also included in the table. From this table we can observe that the quantum efficiencies of Eu^{2+} ions in alkali halides are close to 100%.

Table 1. Relaxation parameters of Eu^{2+} ions in alkali halides.

	NaCl	KCl	KBr	KI
$1 - \alpha$	0.95	0.95	0.91	0.92
Λ	3.7	3.7	3.4	3.5
Φ (%)	102	100	97	99
$\Delta\Phi$ (%)	9	10	11	11

These high values are consistent with the agreement between the calculated and experimental values of the t_{2g} lifetime [15,16], as well as with the reported [17,18] independence of the Eu^{2+} luminescence intensities and lifetime on temperature up to 400 K, indicating a low contribution from the non-radiative channel to the de-excitation.

Let us finally indicate that although the omission of a direct (non-radiative) connection between the upper excited state and the ground state, which was adopted in the previous analysis [7], leads to a slightly overestimated value for the quantum efficiency of Eu^{2+} in KCl (Φ (%) = 104 ± 6), it is almost irrelevant for freshly quenched samples, where aggregates and/or precipitates are absent, and where the values of $(1 - \alpha)$ remain high ($1 - \alpha \approx 1$).

On the other hand, preliminary measurements on precipitated samples indicate that the non-radiative connection between the upper excited state and the ground state is much more important, in accordance with previous luminescence studies [19]. Consequently, α takes substantially higher values, and its omission would lead to physically meaningless high values for the quantum efficiency.

Nevertheless, for precipitated samples the situation becomes even more complicated because of the appearance of different precipitated phases that simultaneously contribute to the photoacoustic signal, and the analysis is not so straightforward as it is for quenched samples. The detailed study of Eu^{2+} precipitated in alkali halides is currently under progress.

Acknowledgments

This work has been partially supported by Agencia Española de Cooperación Internacional, Comisión Interministerial de Ciencia y Tecnología (Spain) under program MAT92-0250, Instituto de Cooperación Iberoamericana (ICI) and the European Community under programme CII*-CT93-0316.

References

- [1] Patel C K N and Tam A C 1981 *Rev. Mod. Phys.* **53** 517
- [2] Tam A C 1986 *Rev. Mod. Phys.* **58** 381

- [3] Vargas H and Miranda L C M 1988 *Phys. Rep.* **161** 43
- [4] Lifante G, Tocho J O and Cusso F 1990 *J. Phys.: Condens. Matter* **2** 3035
- [5] Rothberg L, Jedju T M and Lawrence K 1987 *J. Quant. Spectrosc. Radiat. Transfer* **37** 515
- [6] Dunstan D J 1992 *J. Phys. D: Appl. Phys.* **25** 1825
- [7] Rodriguez E, Tocho J O and Cusso F 1993 *Phys. Rev. B* **47** 14 049
- [8] Diaz J, Cusso F, Jaque F, Lifante G and Da Silva L F 1993 *Phys. Status Solidi a* **139** 549
- [9] Aguirre De Carcer I, Lifante G, Cusso F, Jaque F and Calderon T 1991 *Appl. Phys. Lett.* **58** 1825
- [10] Hernandez J A, Cory W K and Rubio J O 1980 *J. Chem. Phys.* **72** 198
- [11] Braslavsky S E and Heihoff K 1989 *Handbook of Organic Photochemistry* vol 1, ed J C Scaiano (Boca Raton, FL: Chemical Rubber Company) ch 14, pp 327–54
- [12] Murrieta H, Hernandez J and Rubio J 1983 *Kinam* **5** 75
- [13] Merkle L D and Bandyopadhyay P K 1989 *Phys. Rev. B* **39** 6939
- [14] Rodriguez E, Nuñez L, Tocho J O and Cusso F 1994 *J. Lumin.* **58** 53
- [15] Merckle L D and Powell R C 1977 *Chem. Phys. Lett.* **46** 303
- [16] Merckle L D, Powell R C and Wilson T M 1978 *J. Phys. C: Solid State Phys.* **11** 3103
- [17] Jaque F, Hernandez J, Murrieta H and Rubio J 1982 *J. Phys. Soc. Japan* **51** 249
- [18] Muñoz H G, De La Cruz L C, Muñoz F A and Rubio J 1988 *J. Mater. Sci. Lett.* **7** 1310
- [19] Muñoz-Santiuste J E, Garcia-Sole J and Manfredi M 1990 *Phys. Rev. B* **42** 11 339